THE JOURNAL OF PHYSICAL CHEMISTRY B

Article

pubs.acs.org/JPCB

Effect of Alkyl Chain of Room Temperature Ionic Liquid (RTILs) on the Phase Behavior of $[C_2mim][C_nSO_4]$/TX-100/Cyclohexane Microemulsions: Solvent and Rotational Relaxation Study

Surajit Ghosh, Chiranjib Banerjee, Sarthak Mandal, Vishal Govind Rao, and Nilmoni Sarkar*

Department of Chemistry, Indian Institute of Technology, Kharagpur 721302, WB, India

Supporting Information

ABSTRACT: In this investigation, we present microemulsions comprising a nonionic surfactant, Triton X-100 (TX-100), cyclohexane as nonpolar phase, and room temperature ionic liquids (RTILs) as a polar medium. To investigate the effect of alkyl chain length of ionic liquid on the physicochemical properties of microemulsions, we have used 1-ethyl-3-methylimidazolium *n*-butyl sulfate $[C_2mim][C_4SO_4]$, 1-ethyl-3-methylimidazolium *n*-hexyl sulfate $[C_2mim][C_6SO_4]$, and 1-ethyl-3-methylimidazolium *n*-octyl sulfate $[C_2mim][C_8SO_4]$ as polar media. The phase behavior of these ternary systems is investigated by direct observation of transition from clear transparent solution to turbid solution by using UV−vis spectrophotometer at 298 K. The single-phase region is found to increase with increase in chain length of RTIL anion. Dynamic light scattering (DLS) measurements revealed the formation of highly stable nano-sized RTIL-containing microemulsions. The size of the microemulsions increases with the addition of ionic liquid. The maximum increase in size is observed with the addition of $[C_2mim][C_4SO_4]$. It is proposed that the long octyl chain of octyl sulfate allows the anion to align itself along the TX-100 molecules which increases the rigidity of microemulsions, whereas in case of $[C_2mim][C_4SO_4]$, the short butyl chain is apparently unable to do the same. The dynamics of solvent and rotational relaxation of coumarin 480 (C-480) has also been investigated in these ionic liquid containing microemulsions ($[C_2mim][C_4SO_4]$/TX-100/cyclohexane, $[C_2mim][C_6SO_4]$/TX-100/cyclohexane, and $[C_2mim][C_8SO_4]$/TX-100/cyclohexane) using picosecond time-resolved fluorescence spectroscopy. In RTIL microemulsions, solvent relaxation becomes retarded compared to neat RTIL. We have also shown that with increasing *R* value, the solvation dynamics becomes faster and the decrease in average solvation time is more pronounced in $[C_2mim][C_4SO_4]$/TX-100/cyclohexane compared to $[C_2mim][C_6SO_4]$/TX-100/cyclohexane and $[C_2mim][C_8SO_4]$/TX-100/cyclohexane microemulsions.

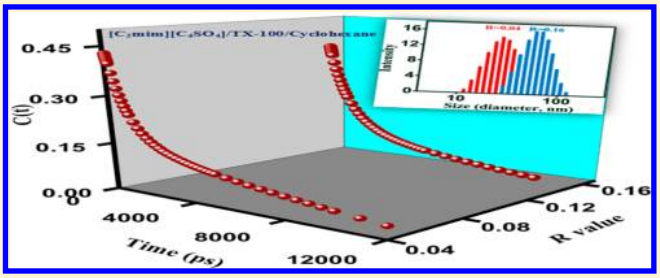

1. INTRODUCTION

Microemulsions are microheterogenous systems where two immiscible liquids, a polar and a nonpolar, are homogeneously mixed due to the presence of an amphiphile (usually a surfactant). Recently, microemulsions have attracted much more attention due to their ability to dissolve polar and nonpolar substances. Thus, these systems are extensively applied in chemical reactions,[1] pharmaceutical industry,[2] nanomaterial synthesis,[3,4] and electrochemistry.[5] There are wide ranges of surfactants that form microemulsions in nonpolar medium where water or other polar solvent is entrapped in the polar core. The nonionic surfactant TX-100 forms microemulsions in cyclohexane without addition of cosurfactant. To study the microemulsions, it is necessary to investigate the phase and swelling behavior. The latter can be detected using dynamic light scattering (DLS) measurement.

In the majority of microemulsions, water is used as polar solvent and the solvent relaxation in these microemulsions has been studied extensively.[6−9] Nonaqueous microemulsions have attracted much more attention.[10−14] Recently, room temperature ionic liquids (RTILs) have been used successfully to replace either water or organic solvents to create microemulsions due to their greater thermal stability as compared to aqueous ones. RTILs are low melting salts composed of bulky organic cations and anions. These are designated as "designer solvent" due to their adjustable solvent properties depending on the combination of ions or on changing the chain length of cation or anion. Their interesting properties, like nonvolatility, suitable polarity, high ionic conductivity, thermal stability, regenerative power, and wide liquidus range,[15−17] make RTILs environment-friendly solvents. Several reports are available in the literature where RTILs are used as reaction media,[18] but their use is restricted due to their inability to dissolve large number of solute molecules. This difficulty can be overcome by using a suitable polar solvent as cosolvent or hydrocarbon domains provided by ionic liquid (IL)-in-oil microemulsions. In the first report, Gao et al.[19] demonstrated that 1-butyl-3-methylimidazolium tetrafluoroborate ($[C_4mim][BF_4]$) could

Received: January 1, 2013
Revised: April 18, 2013

dx.doi.org/10.1021/jp400013r | J. Phys. Chem. B XXXX, XXX, XXX−XXX

form polar nanosized droplets dispersed in cyclohexane/TX-100 system and characterized it by phase behavior study, conductivity measurement, dynamic light scattering measurement, and freeze-fracture electron microscopy. Eastoe et al.[20] have investigated the size and shape of these microemulsions from small-angle neutron scattering (SANS) which showed regular increase in droplet volume with the addition of IL as microemulsions are progressively swollen with added RTIL. It is well reported that surfactant molecules and long-chain ILs also form micelles or microemulsions in neat RTIL or in organic phase.[21−25]

The electrostatic interaction between the $[C_4mim]^+$ ion and the hydrophilic ethylene oxide (EO) groups of TX-100 is the driving force for the formation of ionic liquid containing microemulsions whereas aqueous ones are stabilized by hydrogen bonding between the water molecules and the EO moieties of TX-100.[19,26] Gao and co-workers[26] have investigated the effect of temperature on the microstructure of $[C_4mim][BF_4]$/TX-100/cyclohexane and $[C_4mim][BF_4]$/TX-100/toluene by means of DLS, freeze-fracture transmission electron microscopy (FF-TEM), and two-dimensional rotating frame nuclear overhauser effect (NOE) experiments (ROESY). These systems, due to electrostatic interactions, show high temperature independence and compared to aqueous microemulsions are highly temperature independent. Apart from $[C_4mim][BF_4]$, different RTILs have also been used as water substitutes[27−30] to form microemulsions. Cheng et al.[31] have reported nonaqueous microemulsions using two types of ionic liquids, the hydrophobic ionic liquid $[C_4mim][PF_6]$ as nonpolar medium and the hydrophilic protic ionic liquid propylammonium formate (PAF) as polar medium. Several photophysical and dynamical studies have also been carried out in RTIL micelles and RTIL-containing microemulsions.[32−39]

Koetz et al.[40] investigated the microemulsion formation in the CTAB/IL/toluene system in the presence of cosurfactant pentanol. They used 1-ethyl-3-methylimidazolium ethyl sulfate, $[C_2mim][C_2SO_4]$, and 1-ethyl-3-methylimidazolium hexyl sulfate, $[C_2mim][C_6SO_4]$, as polar core for the characterization of microemulsions. In CTAB/$[C_2mim][C_2SO_4]$/toluene/pentanol microemulsions, when toluene and pentanol ratio is 1:1, unlimited $[C_2mim][C_2SO_4]$ is miscible in the oil mixture. But in CTAB/$[C_2mim][C_6SO_4]$/toluene/pentanol microemulsions, the isotropic phase region is drastically increased at a toluene and pentanol ratio of 15:1. So, it can be concluded that the long chains of RTIL anions are integrated into the interfacial layer of surfactant by attractive ion−ion interaction of the negative head groups of IL−anion and positive headgroup of the cationic surfactant, CTAB. Besides, Wang et al.[41] have reported phase behavior and microstructure of $[C_4mim][PF_6]$, copolymer F127, and H_2O and short-chain alcohols. To investigate the influence of different RTILs on the water solubilization capacity of AOT/isooctane, Wei et al.[42] used three different ionic liquids, $[C_2mim][Cl]$, $[C_4mim][Cl]$, and $[C_8mim][Cl]$. According to these results, the water solubilization capacity is enhanced at low IL concentrations but decreases at high concentrations of IL. But, more interestingly, with increase in alkyl chain, water solubilization capacity also increases at low IL concentrations. RTILs are also used as additives in aqueous micellar solution to tune their physicochemical property. The effect of ionic liquids in modifying properties of different aqueous surfactant solutions has been studied by Pandey and co-workers.[43,44] Previously, we have used $[C_2mim][C_2SO_4]$, $[C_2mim][C_4SO_4]$, and $[C_2mim][C_6SO_4]$ to modify the properties of zwitterionic micelles.[45] A dramatic change in the properties of micelles is observed in case of $[C_2mim][C_6SO_4]$, as the hexyl chain is able to align with the tail part of surfactant. These results showed that the long chain of alcohol or RTIL can align to the surfactant layers and act as cosurfactant.

Keeping this in mind, we have chosen $[C_2mim][C_4SO_4]$, $[C_2mim][C_6SO_4]$, and $[C_2mim][C_8SO_4]$ to maintain a variation in alkyl chain of the anions. Here we intend to explore how the phase behavior and size of nanosized droplet change when these different ILs are incorporated in TX-100/cyclohexane. The solvation dynamics can also provide some useful information on these microemulsions. Extensive studies on solvation dynamics have been done in different heterogeneous media such as micelles, microemulsions, proteins, lipids, etc., using a dipolar molecule for obtaining molecular level information about the response of solvent molecules.[11,38,46−52] Shirota et al.[46] showed that with increase in alkyl chain length of surfactant molecules in aqueous solution, the solvation becomes slower due to the variation of the micellar surface density of the polar headgroup on changing of the alkyl chain length. Samanta and co-workers[53−58] reported solvation dynamics in neat RTIL for the first time. Computer stimulations studies have also been carried out on the structure and dynamics of RTIL to investigate the solvation process. These studies suggest that solvation dynamics in a RTIL involves collective motion of the cations and the anions.[57−63] We have also utilized steady-state and picosecond time-resolved spectroscopy for the investigation of the solvent and rotational relaxation of coumarin 480 in neat $[C_2mim][C_4SO_4]$, $[C_2mim][C_6SO_4]$, $[C_2mim][C_8SO_4]$, and RTIL-containing microemulsions.

2. EXPERIMENTAL SECTION

2.1. Materials. Laser-grade coumarin 480 (C-480) (Exciton) and cyclohexane (Spectrochem, HPLC grade) were used as received. TX-100 was purchased from Sigma-Aldrich and dried in a vacuum oven for 12 h at 343−353 K before use. A stock solution of 0.5 M TX-100 in cyclohexane was prepared by direct weighing. The RTILs, 1-ethyl-3-methylimidazolium ethyl sulfate ($[C_2mim][C_2SO_4]$), 1-ethyl-3-methylimidazolium *n*-butyl sulfate ($[C_2mim][C_4SO_4]$), 1-ethyl-3-methylimidazolium *n*-hexyl sulfate ($[C_2mim][C_6SO_4]$), and 1-ethyl-3-methylimidazolium *n*-octyl sulfate ($[C_2mim][C_8SO_4]$), were obtained from Solvent Innovation GmbH (>98% purity), and were also used as received. The water contents of these ionic liquids are estimated by using digital automatic Karl Fischer Titrator (model VEEGO/MATIC-MD). It was found that the water contents of these ionic liquids are less than 200 ppm. The stock solution of C-480 was prepared in methanol. The RTIL content of the microemulsions solution is expressed by the molar ratio of added RTIL to surfactant i.e.,

$$R = \frac{[\text{RTIL}]}{[\text{TX-100}]} \quad (1)$$

The required amount of the probe was added in a cuvette, and after the methanol was evaporated, TX-100/cyclohexane mixture was added. Then, calculated amounts of ILs were added directly to the TX-100/cyclohexane to get the required *R* value. All the experiments were performed at 298 K.

The structures of coumarin 480 (C-480), TX-100, $[C_2mim][C_nSO_4]$, n = 4, 6, 8, are shown in Scheme 1.

dx.doi.org/10.1021/jp400013r | J. Phys. Chem. B XXXX, XXX, XXX−XXX

Scheme 1. Structures of ILs: 1-Ethyl-3-methylimidazolium *n*-Butyl Sulfate, $[C_2mim][C_4SO_4]$, 1-Ethyl-3-methylimidazolium *n*-Hexyl Sulfate, $[C_2mim][C_6SO_4]$, and 1-Ethyl-3-methylimidazolium *n*-Octyl Sulfate, $[C_2mim][C_8SO_4]$[a]

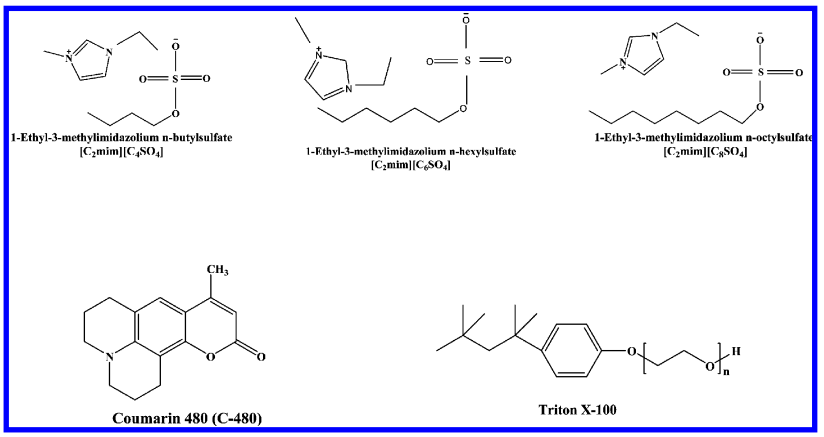

[a]Fluorescence probe, coumarin-480; nonionic surfactant, Triton X-100.

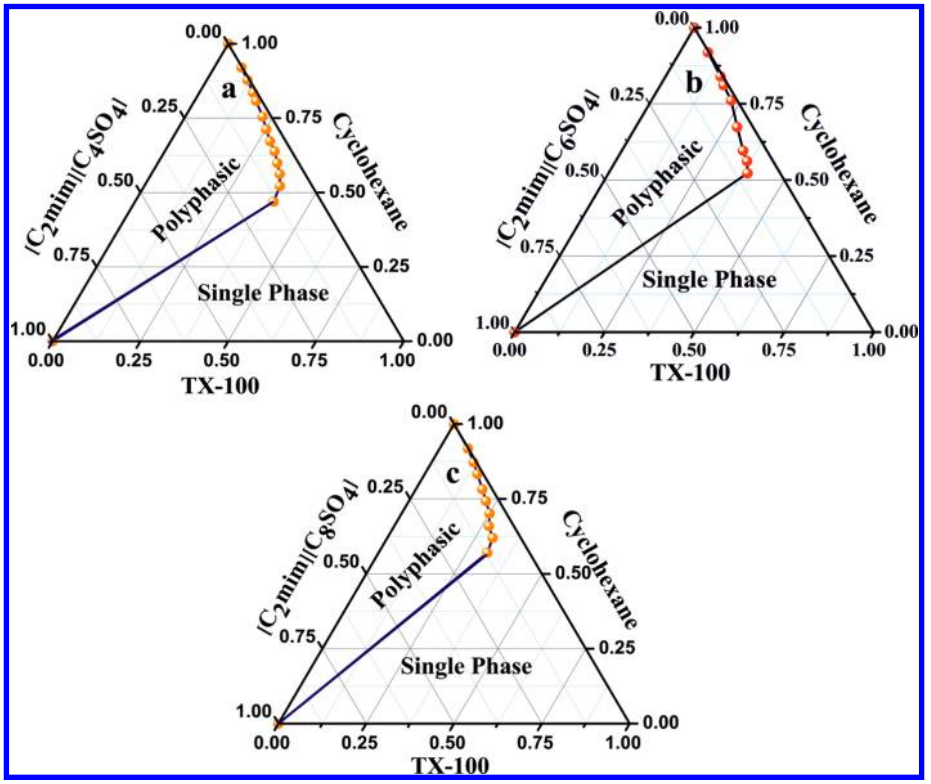

Figure 1. Phase diagrams of the (a) $[C_2mim][C_4SO_4]$/TX-100/cyclohexane, (b) $[C_2mim][C_6SO_4]$/TX-100/cyclohexane, and (c) $[C_2mim][C_8SO_4]$/TX-100/cyclohexane three-component system at 298 K.

2.2. Instrumentation. The absorption and fluorescence spectra were collected using a Shimadzu (model no. UV-2450) spectrophotometer and a Hitachi (model no. F-7000) spectrofluorimeter, respectively. For steady-state measurement, all the samples were excited at 410 nm. Details of the time-resolved fluorescence setup were described in our earlier publication.[64] Briefly, the samples were excited at 410 nm using a picosecond laser diode (IBH, Nanoled), and the signals were collected at the magic angle (54.7°), which is the angle of emission of the polarizer with respect to vertical excitation, using a Hamamatsu microchannel plate photomultiplier tube (3809U). The same setup was used for anisotropy measurements. The instrument response function of our setup is ~100 ps. We used a motorized polarizer on the emission side. The emission intensities at parallel $I_{\parallel}(t)$ and perpendicular $I_{\perp}(t)$ polarizations were collected alternatively until a certain peak difference between parallel $I_{\parallel}(t)$ and perpendicular $I_{\perp}(t)$ decays was reached. When the emission polarizer is oriented parallel to the direction of polarized excitation, the observed intensity is called $I_{\parallel}(t)$. Similarly, when the polarizer is perpendicular to the excitation, the intensity is called $I_{\perp}(t)$. The analysis of the data was done using IBH DAS, version 6, decay analysis software.

We used a Malvern Nano ZS instrument employing a 4 mW He−Ne laser (λ = 632.8 nm) for dynamic light scattering measurements. All of the scattering photons were collected at a 173° scattering angle. The scattering intensity data were processed using the instrumental software to obtain the hydrodynamic diameter (d_h). The instrument measures the

dx.doi.org/10.1021/jp400013r | J. Phys. Chem. B XXXX, XXX, XXX−XXX

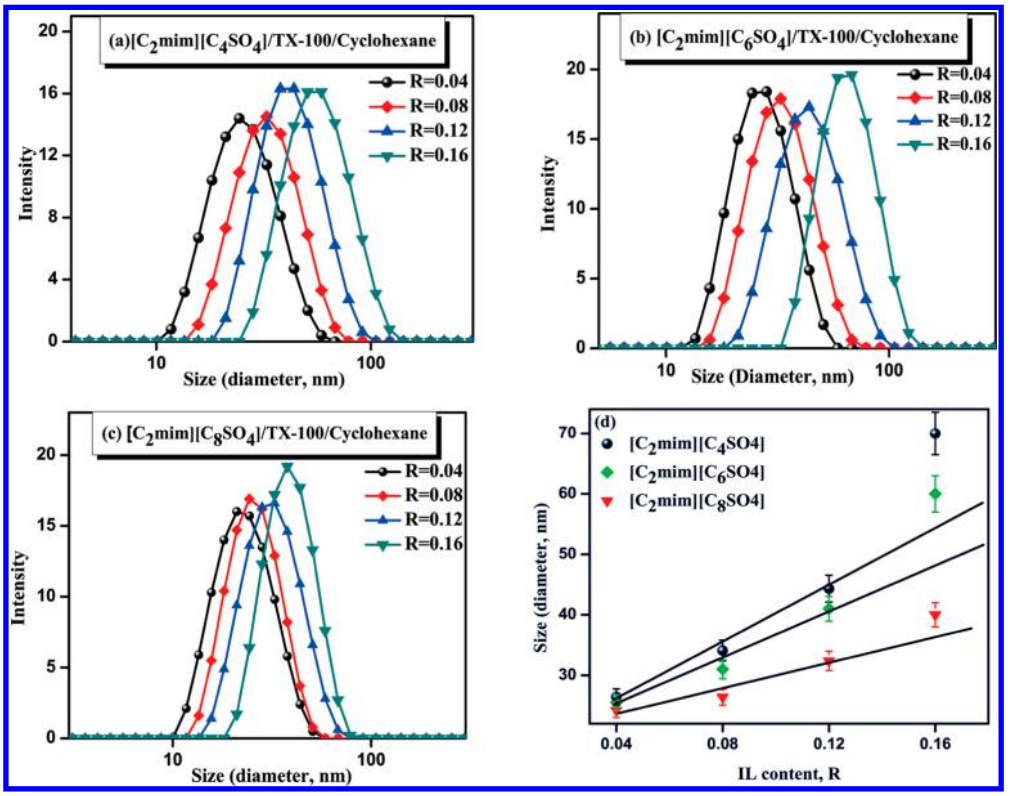

Figure 2. Size (diameter) distribution of the droplets (measured by dynamic light scattering) of (a) $[C_2mim][C_4SO_4]$/TX-100/cyclohexane, (b) $[C_2mim][C_6SO_4]$/TX-100/cyclohexane, (c) $[C_2mim][C_8SO_4]$/TX-100/cyclohexane microemulsions at different R values, and (d) diameter of the droplets of different microemulsions as a function of ILs concentration (R value).

time-dependent fluctuation in the intensity of the light scattered from the particles in solution at a fixed scattering angle and uses this to calculate the average size of particles within the sample. The hydrodynamic diameter (d_h) of the reverse micelle was estimated from the intensity autocorrelation function of the time-dependent fluctuation in intensity. The hydrodynamic diameter (d_h) is defined as

$$d_h = \frac{k_B T}{3\pi\eta D} \quad (2)$$

where k_B is the Boltzmann constant, η is the viscosity, and D is the translational diffusion coefficient. In a typical size distribution graph from the DLS measurement, the x-axis shows a distribution of size classes in nanometers, while the y-axis shows the relative intensity of the scattered light. For viscosity measurements we used a Brookfield DV-II + Pro (viscometer) at 298 K.

3. RESULTS AND DISCUSSION

3.1. Phase Behavior Study. Phase behavior study is an essential step for the characterization of microemulsions and surfactant solutions. In this work, we have used TX-100 as surfactant, cyclohexane as nonpolar solvent, and $[C_2mim][C_4SO_4]$, $[C_2mim][C_6SO_4]$, and $[C_2mim][C_8SO_4]$ as ionic liquids. We have characterized the partial phase diagram of the ternary system of $[C_2mim][C_4SO_4]$/TX-100/cyclohexane, $[C_2mim][C_6SO_4]$/TX-100/cyclohexane, and $[C_2mim][C_8SO_4]$/TX-100/cyclohexane at 298 K. The phase boundary was determined by observing the change of the sample appearance from transparent to turbid, by using UV−vis spectrophotometer (Figure 1). We measured the transmittance of the solutions at 650 nm, visible region. The plot of turbidity versus weight fraction of the ionic liquid $[C_2mim][C_6SO_4]$ for TX-100/cyclohexane is given in Figure S1 (Supporting Information). As depicted in Figure 1, two different regions are observed, a poly phase region and a single phase region. The region marked as "single phase" is transparent and "polyphase" region is the turbid one. For these systems, a continuous stable single-phase microemulsion region can always be observed. It is observed that for $[C_2mim][C_8SO_4]$/TX-100/cyclohexane system the area of single-phase region is larger compared to other microemulsions and follows the trend $[C_2mim][C_8SO_4]$/TX-100/cyclohexane > $[C_2mim][C_6SO_4]$/TX-100/cyclohexane > $[C_2mim][C4SO_4]$/TX-100/cyclohexane. So, it is concluded that, with the increase in alkyl chain of RTIL, the polyphasic region decreases. To investigate the influence of chain length of the RTIL anion in the formation of microemulsions, the same experiment was done using 1-ethyl-3-methylimidazolium ethyl sulfate, $[C_2mim][C_2SO_4]$. However, it is observed that $[C_2mim][C_2SO_4]$ is unable to form microemulsions in TX-100/cyclohexane.

In $[C_2mim][C_8SO_4]$/TX-100/cyclohexane microemulsion, the octyl sulfate anions can also act as cosurfactant due to its long octyl chain, which align in interfacial layers of TX-100. So, besides interaction between the $[C_2mim]^+$ ion and the hydrophilic EO groups of TX-100, the hydrophobic interaction between the alkyl part of RTIL and the TX-100 molecules is the main driving force for formation of this microemulsion. $[C_2mim][C_2SO_4]$ is unable to form microemulsions in the TX-100/cyclohexane system due to the absence of alkyl chain. The pronounced penetration and alignment of $[C_8SO_4]$ anion with the tail part of TX-100 makes the interfacial layer more rigid, which increases solubilization capacity of RTIL and increases

dx.doi.org/10.1021/jp400013r | J. Phys. Chem. B XXXX, XXX, XXX−XXX

the single-phase region. So, this proposed statement is in agreement with our other experimental findings.

3.2. Dynamic Light Scattering Measurements. Dynamic light scattering (DLS) measurement is a powerful technique to evaluate the size and size distribution of microemulsions. If the ILs are encapsulated by the surfactant to create the microemulsions, the droplet size must increase as the R value increases. The size distribution and variation of size with increasing R value for $[C_2mim][C_4SO_4]$/TX-100/cyclohexane, $[C_2mim][C_6SO_4]$/TX-100/cyclohexane, and $[C_2mim]$-$[C_8SO_4]$/TX-100/cyclohexane systems are shown in Figure 2 which clearly indicates the swelling behavior of IL-in-oil microemulsions with the addition of ILs. This swelling behavior of the droplets (linearly with increasing R value) clearly shows that the microemulsion media consist of discrete spherical and noninteracting droplets of ILs stabilized by the TX-100.[65] The deviation at higher R value is due to several reasons, the most relevant ones being increased droplet−droplet interaction and shape of the microemulsions. The size of the aggregates increases from ∼24 to ∼42 nm for the $[C_2mim][C_8SO_4]$/TX-100/cyclohexane system on increasing the R value from 0.04 to 0.16. The trend in size change for the $[C_2mim][C_4SO_4]$/TX-100/cyclohexane microemulsions is larger compared to $[C_2mim][C_8SO_4]$/TX-100/cyclohexane. For $[C_2mim]$-$[C_4SO_4]$/TX-100/cyclohexane, the size of aggregates increases from ∼26 to ∼70 nm, and for $[C_2mim][C_6SO_4]$/TX-100/cyclohexane, it increases from ∼25 to ∼60 nm. The sizes of these microemulsions with increasing R value are listed in Table 1. We observed almost linear relationship between size and R value for these three microemulsions (Figure 2d). We have mentioned earlier that the presence of octyl chain in $[C_2mim][C_8SO_4]$ causes more penetration as compared to $[C_2mim][C_4SO_4]$ and $[C_2mim][C_6SO_4]$, due to alignment of $[C_8SO_4]$ anions in the interfacial regions of TX-100 molecules. As a result, this cosurfactant nature of octyl sulfate increases the rigidity of $[C_2mim][C_8SO_4]$/TX-100/cyclohexane as compared to the other two microemulsions. As large numbers of $[C_8SO_4]$ anions are integrated in the interfacial regions of TX-100 molecules, so the swelling behavior of $[C_2mim][C_8SO_4]$/TX-100/cyclohexane microemulsions is lesser than that of $[C_2mim][C_4SO_4]$/TX-100/cyclohexane and $[C_2mim]$-$[C_6SO_4]$/TX-100/cyclohexane microemulsions.

Table 1. Size (Diameter) of the $[C_2mim][C_8SO_4]$/TX-100/Cyclohexane, $[C_2mim][C_6SO_4]$/TX-100/Cyclohexane, and $[C_2mim][C_4SO_4]$/TX-100/Cyclohexane Microemulsions at Different R Values

system	R = [RTIL]/[TX-100]	size (nm)
$[C_2mim][C_8SO_4]$/TX-100/cyclohexane	R = 0.04	24 ± 1
	R = 0.08	26 ± 2
	R = 0.12	34 ± 2
	R = 0.16	42 ± 3
$[C_2mim][C_6SO_4]$/TX-100/cyclohexane	R = 0.04	25 ± 1
	R = 0.08	31 ± 1
	R = 0.12	41 ± 2
	R = 0.16	60 ± 3
$[C_2mim][C_4SO_4]$/TX-100/cyclohexane	R = 0.04	26 ± 2
	R = 0.08	34 ± 2
	R = 0.12	45 ± 3
	R = 0.16	70 ± 4

3.3. Steady-State Studies. Steady-state absorption and emission spectra of a solvatochromic molecule provide some valuable information about the location of the molecules in microemulsions. The representative absorption and emission spectra of C-480 in neat $[C_2mim][C_8SO_4]$, $[C_2mim][C_6SO_4]$, and $[C_2mim][C_4SO_4]$ are shown in Figure 3. The emission maxima of C-480 in $[C_2mim][C_8SO_4]$, $[C_2mim][C_6SO_4]$, and $[C_2mim][C_4SO_4]$ are respectively ∼461, ∼463, and ∼466 nm. This blue shift in absorption and emission maxima of C-480 on going from $[C_2mim][C_4SO_4]$ to $[C_2mim][C_8SO_4]$ is due to appreciable increase in the nonpolar character of the ILs with increasing alkyl chain length. The absorption and emission maxima of C-480 in cyclohexane are respectively ∼361 and ∼409 nm (λ_{ex} = 375 nm). On the addition of TX-100 to cyclohexane the absorption and emission maxima of C-480 get red-shifted to ∼373 and ∼451 nm, respectively. This red shift in the emission by ∼42 nm indicates the migration of probe molecules from bulk cyclohexane to TX-100/cyclohexane mixture. With the addition of IL, $[C_2mim][C_4SO_4]$, $[C_2mim]$-$[C_6SO_4]$, and $[C_2mim][C_8SO_4]$, further red shift is observed in the emission spectra (Figure 4). The absorption spectra at the red end side gradually increases with the addition of ionic liquids to the TX-100/cyclohexane system. This indicates migration of probe molecules to RTIL pool of microemulsions. The absorption spectra of C-480 in $[C_2mim][C_4SO_4]$/TX-100/cyclohexane and $[C_2mim][C_8SO_4]$/TX-100/cyclohexane are given in Figure S2 (Supporting Information). These results are summarized in Table 2.

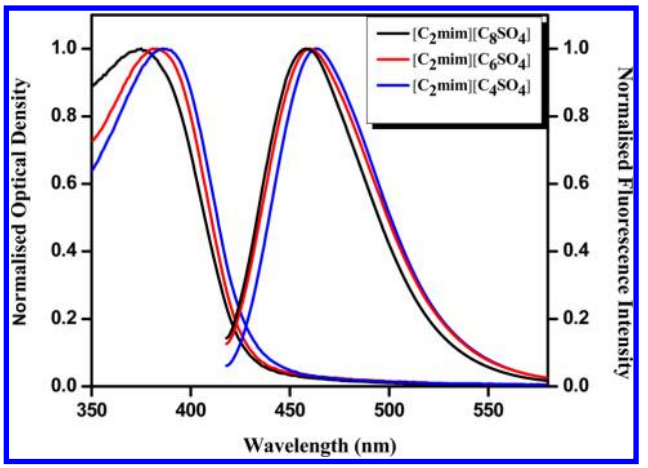

Figure 3. Absorption and emission spectra of C-480 in $[C_2mim]$-$[C_8SO_4]$, $[C_2mim][C_6SO_4]$, and $[C_2mim][C_4SO_4]$.

3.4. Time-Resolved Studies. *3.4.1. Time-Resolved Anisotropy Studies.* Time-resolved anisotropy measurement provides valuable information about the location of probe molecule in a system. The time-resolved fluorescence anisotropy, $r(t)$, is calculated using the following equation

$$r(t) = \frac{I_{\parallel}(t) - GI_{\perp}(t)}{I_{\parallel}(t) + 2GI_{\perp}(t)} \quad (3)$$

where G is the instrument correction factor of the detector sensitivity to the polarization direction of the emission, which is 0.6 for our instrumental set up. $I_{\parallel}(t)$ and $I_{\perp}(t)$ are fluorescence decays polarized parallel and perpendicular to the polarization of the excitation light, respectively.

dx.doi.org/10.1021/jp400013r | J. Phys. Chem. B XXXX, XXX, XXX−XXX

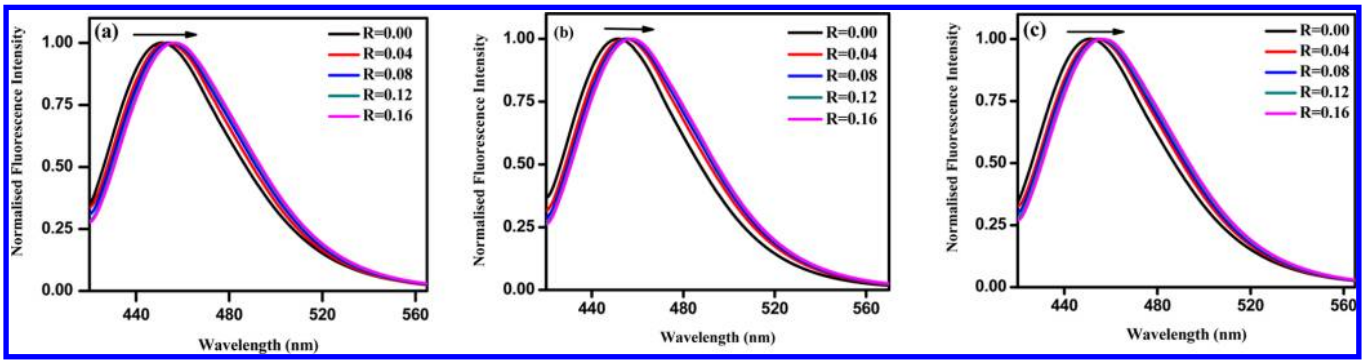

Figure 4. Emission spectra of C-480 in (a) $[C_2mim][C_4SO_4]$/TX-100/cyclohexane, (b) $[C_2mim][C_6SO_4]$/TX-100/cyclohexane, and (c) $[C_2mim][C_8SO_4]$/TX-100/cyclohexane at different R values.

Table 2. Steady-State Absorption and Emission maxima of C-480 in Neat $[C_2mim][C_8SO_4]$, $[C_2mim][C_6SO_4]$, and $[C_2mim][C_4SO_4]$, and $[C_2mim][C_8SO_4]$/TX-100/ Cyclohexane, $[C_2mim][C_6SO_4]$/TX-100/Cyclohexane, and $[C_2mim][C_4SO_4]$/TX-100/Cyclohexane Microemulsions

system	λ_{abs}^{max} (nm)	λ_{em}^{max} (nm)
TX-100/cyclohexane	373	451
neat $[C_2mim][C_8SO_4]$	376	461
$[C_2mim][C_8SO_4]$/TX-100/cyclohexane (R = 0.04)	373	454
$[C_2mim][C_8SO_4]$/TX-100/cyclohexane (R = 0.08)	373	455
$[C_2mim][C_8SO_4]$/TX-100/cyclohexane (R = 0.12)	373	456
$[C_2mim][C_8SO_4]$/TX-100/cyclohexane (R = 0.16)	374	457
neat $[C_2mim][C_6SO_4]$	381	463
$[C_2mim][C_6SO_4]$/TX-100/cyclohexane (R = 0.04)	373	454
$[C_2mim][C_6SO_4]$/TX-100/cyclohexane (R = 0.08)	373	456
$[C_2mim][C_6SO_4]$/TX-100/cyclohexane (R = 0.12)	374	457
$[C_2mim][C_6SO_4]$/TX-100/cyclohexane (R = 0.16)	374	458
neat $[C_2mim][C_4SO_4]$	384	466
$[C_2mim][C_4SO_4]$/TX-100/cyclohexane (R = 0.04)	374	454
$[C_2mim][C_4SO_4]$/TX-100/cyclohexane (R = 0.08)	374	456
$[C_2mim][C_4SO_4]$/TX-100/cyclohexane (R = 0.12)	374	457
$[C_2mim][C_4SO_4]$/TX-100/cyclohexane (R = 0.16)	375	459

The representative anisotropy decay profiles of C-480 in neat $[C_2mim][C_8SO_4]$ and $[C_2mim][C_4SO_4]$ are shown in Figure S3 (Supporting Information). The anisotropy decays in microemulsions are fitted with a biexponential function. The anisotropy decays of C-480 in the presence and absence of ionic liquid are different. The anisotropy decay of probe molecules in TX-100/cyclohexane is single exponential with a time constant ~80 ps (Figure S4, Supporting Information). With the addition of $[C_2mim][C_8SO_4]$, $[C_2mim][C_6SO_4]$, and $[C_2mim][C_4SO_4]$ to TX-100/cyclohexane, the rotational time constant increases with the emergence of an additional slow component (biexponential in nature). The anisotropy decay parameters are listed in Table 3. The average rotational relaxation time for C-480 in $[C_2mim][C_8SO_4]$/TX-100/ cyclohexane microemulsions increases from ~1.04 to ~1.42 ns whereas in the $[C_2mim][C_4SO_4]$/TX-100/cyclohexane system it increases from ~0.93 to ~1.22 ns at R = 0.04 to R = 0.16, respectively. The high rotational relaxation times in the presence of ionic liquid indicate that the probe molecules experience a different environment inside the ionic liquid pool of the microemulsions than in the TX-100/cyclohexane mixture. Since with the addition of RTIL to microemulsions the viscosity of the RTIL pool increases, the average rotational relaxation time also increases.

Table 3. Anisotropy Decay Parameters of C-480 in Neat $[C_2mim][C_8SO_4]$, $[C_2mim][C_8SO_4]$/TX-100/Cyclohexane, Neat $[C_2mim][C_6SO_4]$, $[C_2mim][C_6SO_4]$/TX-100/Cyclohexane, Neat $[C_2mim][C_4SO_4]$, and $[C_2mim][C_4SO_4]$/TX-100/ Cyclohexane Microemulsions Different R Values

system	R = [RTIL]/[TX-100]	a_{slow}	τ_{slow} (ns)	a_{fast}	τ_{fast} (ns)	$\langle\tau_{rot}\rangle$ (ns)	viscosity (cP)
TX-100/cyclohexane		1.00	0.08			0.08	4.98
neat $[C_2mim][C_8SO_4]$		0.74	5.67	0.26	0.93	4.44 ± 0.20	351
$[C_2mim][C_8SO_4]$/TX-100/cyclohexane	R = 0.04	0.40	1.87	0.60	0.49	1.04 ± 0.05	6.05
	R = 0.08	0.52	1.97	0.48	0.41	1.22 ± 0.06	7.50
	R = 0.12	0.54	1.99	0.46	0.46	1.24 ± 0.06	9.00
	R = 0.16	0.44	2.56	0.56	0.50	1.41 ± 0.07	11.00
neat $[C_2mim][C_6SO_4]$		0.76	5.10	0.26	0.81	4.08 ± 0.18	195
$[C_2mim][C_6SO_4]$/TX-100/cyclohexane	R = 0.04	0.42	1.79	0.58	0.41	1.02 ± 0.04	5.50
	R = 0.08	0.49	1.94	0.51	0.39	1.15 ± 0.05	6.75
	R = 0.12	0.50	2.12	0.50	0.42	1.27 ± 0.06	7.98
	R = 0.16	0.53	2.16	0.47	0.44	1.36 ± 0.07	9.00
neat $[C_2mim][C_4SO_4]$		0.77	4.05	0.23	0.60	3.25 ± 0.16	115
$[C_2mim][C_4SO_4]$/TX-100/cyclohexane	R = 0.04	0.41	1.64	0.59	0.44	0.93 ± 0.04	5.10
	R = 0.08	0.51	1.71	0.49	0.40	1.07 ± 0.05	5.68
	R = 0.12	0.56	1.73	0.44	0.36	1.13 ± 0.06	6.50
	R = 0.16	0.53	1.94	0.47	0.40	1.22 ± 0.06	7.50

dx.doi.org/10.1021/jp400013r | J. Phys. Chem. B XXXX, XXX, XXX–XXX

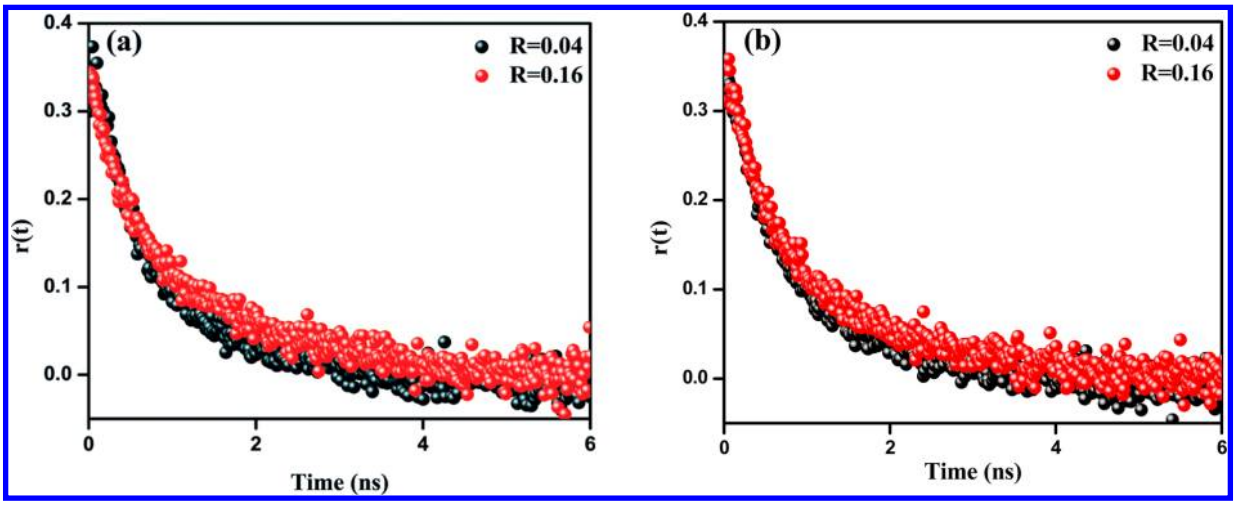

Figure 5. Anisotropy decays of C-480 in (a) $[C_2mim][C_4SO_4]$/TX-100/cyclohexane and (b) $[C_2mim][C_8SO_4]$/TX-100/cyclohexane at R = 0.04 and R = 0.16.

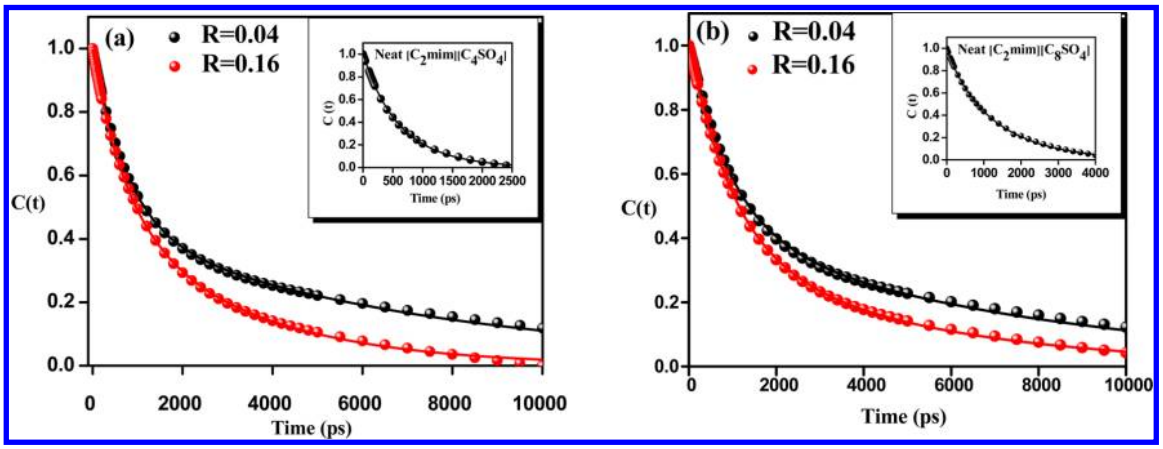

Figure 6. Decay of solvent correlation function $C(t)$ of C-480 in (a) $[C_2mim][C_4SO_4]$/TX-100/cyclohexane and (b) $[C_2mim][C_8SO_4]$/TX-100/cyclohexane at R = 0.04 and R = 0.16.

In neat $[C_2mim][C_4SO_4]$, $[C_2mim][C_6SO_4]$, and $[C_2mim][C_8SO_4]$, C-480 exhibits very slow rotational dynamics with an average time constant ~3.25, ~4.08, and ~4.44 ns, respectively. This slow anisotropy value is due to their high viscosities (viscosities of $[C_2mim][C_4SO_4]$, $[C_2mim][C_6SO_4]$, and $[C_2mim][C_8SO_4]$ are ~115, ~ 195, and ~351 cP, respectively). In TX-100/cyclohexane the rotational time constant is very fast (80 ps). In $[C_2mim][C_4SO_4]$/TX-100/cyclohexane microemulsions, at R = 0.04, we obtained an average anisotropy value of ~0.93 ns. With increasing R value (at R = 0.16), the viscosity of RTIL pool increases, and so we got a higher anisotropy value of ~1.22 ns. In the case of $[C_2mim][C_8SO_4]$/TX-100/cyclohexane microemulsions, at R = 0.16, the constraint effect is maximum due to smaller reverse micellar size. We got higher anisotropy value of ~1.41 ns in this condition. The representative anisotropy decays are shown in Figure 5. Thus, with increasing R value (addition of $[C_2mim][C_4SO_4]$, $[C_2mim][C_6SO_4]$, and $[C_2mim][C_8SO_4]$, from R = 0.04 to R = 0.16) in TX-100 reverse micelle, anisotropy value increases by ~31%, ~33%, and ~36% respectively. This high increase in anisotropy for $[C_2mim][C_8SO_4]$/TX-100/cyclohexane microemulsions is due to a small increase in its size with the addition of ILs. The representative anisotropy decays for $[C_2mim][C_6SO_4]$/TX-100/cyclohexane at R = 0.04 and R = 0.16 are shown in Figure S5a in the Supporting Information.

3.4.2. Solvation Dynamics. Steady-state absorption and emission spectra of C-480 in $[C_2mim][C_8SO_4]$/TX-100/cyclohexane and $[C_2mim][C_4SO_4]$/TX-100/cyclohexane system provide important information about the probe location inside the microemulsions. To study the solvation relaxation dynamics in these systems, we have collected the time-resolved decays monitored at different wavelengths over the emission spectra. The fluorescence decays at the red edge of emission spectra consist of a clear rise (growth) followed by usual decay and at the blue end of emission spectra a faster decay is observed. This wavelength-dependent behavior of the decays of C-480 clearly indicates that solvation is occurring in these systems. The representative decays of C-480 in $[C_2mim][C_8SO_4]$/TX-100/cyclohexane and $[C_2mim][C_4SO_4]$/TX-100/cyclohexane at R = 0.16 are shown in Figure S6 (Supporting Information). The time-resolved emission spectra (TRES) were constructed using the procedure of Fleming and Maroncelli.[66] The TRES at a given time t, $S(\lambda;t)$, is obtained by the fitted decays, $D(t;\lambda)$, by relative normalization to the steady-state spectrum $S_0(\lambda)$, as follows

dx.doi.org/10.1021/jp400013r | J. Phys. Chem. B XXXX, XXX, XXX−XXX

$$S(\lambda; t) = D(\lambda; t)\frac{S_0(\lambda)}{\int_0^\infty D(\lambda; t)\, dt} \quad (4)$$

Each (TRES) was fitted by a "log-normal line shape function", which is defined as

$$g(\nu) = g_0 \exp\left[(-\ln 2)\left(\frac{\ln[1 + 2b(\nu - \nu_p)/\Delta]}{b}\right)^2\right] \quad (5)$$

where g_0, b, ν_p, and Δ are the peak height, asymmetric parameter, peak frequency, and width parameter, respectively. The representative TRES plots of C-480 in $[C_2mim][C_8SO_4]$/TX-100/cyclohexane and $[C_2mim][C_4SO_4]$/TX-100/cyclohexane at R = 0.16 are shown in Figure S7 (Supporting Information). We have calculated the peak frequency from the log-normal fitting of TRES. This peak frequency is used to construct the decay of the solvent correlation function $C(t)$, which is defined as

$$C(t) = \frac{\nu(t) - \nu(\infty)}{\nu(0) - \nu(\infty)} \quad (6)$$

where $\nu(0)$, $\nu(t)$, and $\nu(\infty)$ are the peak frequency at time zero, t, and infinity. The decays of $C(t)$ are fitted by a biexponential function

$$C(t) = a_1 \exp^{-t/\tau_1} + a_2 \exp^{-t/\tau_2} \quad (7)$$

where τ_1 and τ_2 are the solvation times with amplitudes of a_1 and a_2, respectively.

The $C(t)$ versus time plots for $[C_2mim][C_4SO_4]$/TX100/cyclohexane and $[C_2mim][C_8SO_4]$/TX-100/cyclohexane microemulsions at R = 0.04 and R = 0.16 are shown in Figure 6. The average lifetime ($\langle\tau_s\rangle$) is calculated using the following equation:

$$\langle\tau_s\rangle = a_1\tau_1 + a_2\tau_2 \quad (8)$$

Before we describe the solvent relaxation results in $[C_2mim][C_8SO_4]$/TX-100/cyclohexane and $[C_2mim][C_4SO_4]$/TX-100/cyclohexane microemulsions, some distinct features of solvation dynamics in RTIL are discussed here. The solvation process in neat RTIL is quite different from that in conventional polar solvents, such as water, methanol, or acetonitrile. The solvation process in conventional polar solvents is extremely fast (subpicosecond or picosecond time scale) whereas in neat RTIL solvation takes place in picosecond to nanosecond time scale.[67] Chapman and Maroncelli[68] also showed that the ionic solvation is slower compared to pure solvent. The motions of the cations and anions around the photoexcited dipolar molecules are responsible for the solvation in neat RTIL while in polar solvents solvation takes place as the solvent molecules reorient themselves around the excited dye. There are many reports depicting the biphasic nature of solvation process in RTIL.[62,63,69−72] Samanta et al. demonstrated that the fast component arises due to the motion of anions whereas the slow component arises due to collective motions of both anions and cations.[53−56,73]

To comprehend the solvation dynamics results in the microemulsions system, the location of the probe molecules within the microemulsions is necessary. Absorption, emission, and anisotropy measurements demonstrated that substantial numbers of probe molecules are present in the core of microemulsions. The solvent relaxation times observed from the solvent correlation function $C(t)$ are tabulated in Table 4. The average solvation time of C-480 in neat $[C_2mim][C_8SO_4]$, $[C_2mim][C_6SO_4]$, and neat $[C_2mim][C_4SO_4]$ are ∼1.26, ∼1.09, and ∼0.64 ns, respectively. The increase in average solvation times with increasing the alkyl chain length is due to increase in bulk viscosity of the medium. When these ionic liquids are incorporated into the TX-100/cyclohexane, the average solvation time increases. The average solvation times of C-480 in $[C_2mim][C_4SO_4]$/TX-100/cyclohexane, $[C_2mim][C_6SO_4]$/TX-100/cyclohexane and $[C_2mim][C_8SO_4]$/TX-100/cyclohexane microemulsions at R = 0.04 becomes ∼5.27, ∼4.71, and ∼4.54 ns, respectively. These increases in average solvation times of C-480 in RTIL microemulsions can be explained by the nanocage confinement of RTIL inside the microemulsions core and interaction of RTIL with headgroup of TX-100. On addition of further ionic liquids in TX100/cyclohexane reverse micelle, the solvent relaxation of C-480 becomes faster. At different R values, we observed a biexponential nature of solvation dynamics in these microemulsions.

The average solvation time of C-480 in $[C_2mim][C_8SO_4]$/TX-100/cyclohexane at R = 0.04 is ∼5.27 ns, consisting of time constants of the fast component as ∼0.97 ns (with relative

Table 4. Decay Parameters of $C(t)$ of C-480 in Neat $[C_2mim][C_8SO_4]$, $[C_2mim][C_8SO_4]$/TX-100/Cyclohexane, Neat $[C_2mim][C_6SO_4]$, $[C_2mim][C_6SO_4]$/TX-100/Cyclohexane, Neat $[C_2mim][C_4SO_4]$, and $[C_2mim][C_4SO_4]$/TX-100/Cyclohexane Microemulsions Different R Values

system	R = [RTIL]/[TX-100]	τ_i (a_i) (ns)	$\langle\tau_s\rangle^a$ (ns)	missing component (%)
neat $[C_2mim][C_8SO_4]$		1.37 (0.89), 0.34 (0.11)	1.26 ± 0.06	59
$[C_2mim][C_8SO_4]$/TX-100/cyclohexane	R = 0.04	10.32 (0.46), 0.97 (0.54)	5.27 ± 0.15	50
	R = 0.08	9.12 (0.47), 1.14 (0.53)	4.89 ± 0.13	52
	R = 0.12	8.50 (0.45), 1.09 (0.55)	4.42 ± 0.13	53
	R = 0.16	8.22 (0.42), 1.05 (0.58)	4.06 ± 0.12	53
neat $[C_2mim][C_6SO_4]$		1.14 (0.92), 0.54 (0.08)	1.09 ± 0.05	62
$[C_2mim][C_6SO_4]$/TX-100/cyclohexane	R = 0.04	9.81 (0.43), 0.86 (0.57)	4.71 ± 0.13	52
	R = 0.08	8.66 (0.41), 0.94 (0.59)	4.11 ± 0.12	53
	R = 0.12	7.35 (0.44), 0.95 (0.56)	3.77 ± 0.11	53
	R = 0.16	6.35 (0.44), 0.94 (0.56)	3.32 ± 0.10	54
neat $[C_2mim][C_4SO_4]$		0.70 (0.84), 0.33 (0.16)	0.64 ± 0.04	64
$[C_2mim][C_4SO_4]$/TX-100/cyclohexane	R = 0.04	9.31 (0.44), 0.79 (0.56)	4.54 ± 0.13	51
	R = 0.08	7.61 (0.46), 0.85 (0.54)	3.96 ± 0.12	53
	R = 0.12	7.27 (0.42), 0.98 (0.58)	3.62 ± 0.11	54
	R = 0.16	5.63 (0.42), 0.86 (0.58)	2.86 ± 0.08	56

$^a\langle\tau_s\rangle = \alpha_1\tau_1 + \alpha_2\tau_2$.

dx.doi.org/10.1021/jp400013r | J. Phys. Chem. B XXXX, XXX, XXX−XXX

contribution of 54%) and the slow component as ~10.32 ns (with relative contribution of 46%) and with increase in R value (R = 0.16) the average solvation time becomes ~4.06 ns (with relative contribution ~1.05 and ~8.22 ns). Similar observation is obtained for $[C_2mim][C_6SO_4]$/TX-100/cyclohexane and $[C_2mim][C_4SO_4]$/TX-100/cyclohexane microemulsions (Table 4).

Shirota et al.[46] have showed that, in micellar solution, the solvation dynamics of C-480 is retarded with increasing alkyl chain length of surfactant molecules. In comparison between the cationic alkyltrimethylammonium bromide and anionic sodium alkyl sulfate surfactants of the same alkyl chain length, the slower solvation dynamics in the anionic micellar solution is observed due to stronger hydration of the anionic sulfate group compared to the cationic alkyltrimethylammonium moiety. In our system, different RTILs have the same cation but anion is different in alkyl chain length. In correlation with that, the average solvation time of C-480 also increases in neat RTIL and RTIL forming microemulsions with an increase in the alkyl chain length of RTIL anion. In $[C_2mim][C_8SO_4]$/TX-100/cyclohexane, the strong hydrophobic interaction between $[C_8SO_4]$ anions and tail part of TX-100 molecules results in a small increase in size and consequently the solvation time becomes larger compared with other two microemulsions, $[C_2mim][C_4SO_4]$/TX-100/cyclohexane and $[C_2mim]$-$[C_6SO_4]$/TX-100/cyclohexane. The average solvation time of C-480 in micellar solution remains almost unchanged with an increase in surfactant concentration as previously reported by Shirota et al.[74] On increasing the surfactant concentration, the number of micelles in water increases, which eventually increases the observed solvation component. But in microemulsions, as R value increases, the amount of ionic liquid in the pool of microemulsion also increases, which results in a faster solvation process. Moreover, an interesting point to note is that the relative contributions of fast and slow component remain almost the same irrespective of the alkyl chain length of surfactant molecules in micellar solution. In addition to this, the relative contributions of fast and slow component are almost same with the variation of alkyl chain length of ionic liquids in RTIL forming microemulsions.

With gradual increase in R value from 0.04 to 0.16, the average solvation time (Table 4) decreases from ~5.27 to ~4.06 ns in $[C_2mim][C_8SO_4]$/TX-100/cyclohexane, from ~4.71 to ~3.32 ns in $[C_2mim][C_6SO_4]$/TX-100/cyclohexane, and from ~4.54 to ~2.86 ns in $[C_2mim][C_4SO_4]$/TX-100/cyclohexane. So, with increase in size of microemulsions, the RTIL becomes less confined; as a result, average solvation time decreases. A close inspection of the observed size with increase in R value of the microemulsions indicates that the solvation times largely depend on size of microemulsions. It has been observed that with addition of RTIL to TX-100/cyclohexane solvation dynamics becomes faster and the change in solvation dynamics is more pronounced in the case of $[C_2mim][C_4SO_4]$ compared to that for $[C_2mim][C_8SO_4]$. From DLS measurement, it is observed that the size of $[C_2mim][C_4SO_4]$-containing microemulsions increases more than $[C_2mim]$-$[C_6SO_4]$- and $[C_2mim][C_8SO_4]$-containing microemulsions. Variations in average solvation time ($\langle\tau_s\rangle$) of C-480 with the size of microemulsions are shown in Figure 7. In the case of $[C_2mim][C_4SO_4]$/TX-100/cyclohexane, ~37% decrease in average solvation time is observed but in $[C_2mim][C_8SO_4]$/TX-100/cyclohexane and $[[C_2mim][C_6SO_4]$/TX-100/cyclohexane the decrease in solvation time is less, only ~23% and 30%, respectively, from R = 0.04 to R = 0.16.

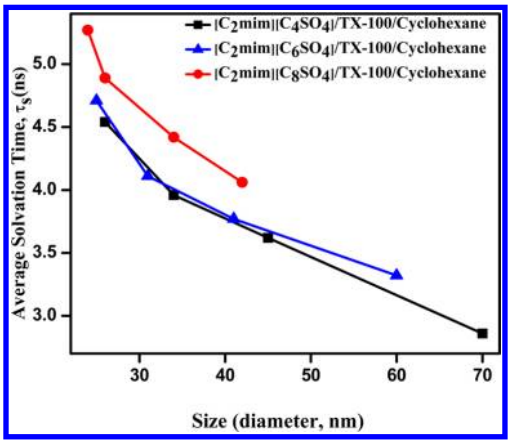

Figure 7. Variation of solvation time (τ_s) of the droplets of the microemulsions as a function of size (diameter).

In this study using the TCSPC setup, we are missing the fast component of the solvation dynamics (<100 ps). Here, we have applied the method of Fee and Maroncelli[75] to calculate the missing component. We have calculated a "time zero spectrum" using the above procedure. The time zero frequency can be estimated using the following relation from absorption and emission spectra:

$$\nu_p(t=0) \approx \nu_p(\text{abs}) - [\nu_{np}(\text{abs}) - \nu_{np}(\text{em})] \quad (9)$$

where the subscripts "p" and "np" refer to the spectra in polar and nonpolar solvents, respectively. The percentage of missing component is $[\nu_{cal}(0) - \nu(0)]/[\nu_{cal}(0) - \nu(\infty)] \times 100$. Using C-480 as experimental probe, we have calculated a total Stokes' shift of ~1769 cm^{-1}, but we have observed a total Stokes' shift of ~721 cm^{-1} for neat $[C_2mim][C_8SO_4]$. This suggests that ~59% of the dynamics is missed due to the limited resolution of our TCSPC setup. The missing components of neat RTIL and RTIL-containing microemulsions for all R values are tabulated in Table 4. As depicted in Table 4, the percentage of the missing component decreases for all the microemulsions compared to that of neat RTIL. This result also indicates the slow solvation of RTIL in microemulsions compared to that of neat ones.

4. CONCLUSION

We have explored the formation of nonaqueous microemulsions by using $[C_2mim][C_4SO_4]$, $[C_2mim][C_6SO_4]$, and $[C_2mim][C_8SO_4]$ as polar phase in the presence of cyclohexane as nonpolar phase and TX-100 as surfactant. Phase behavior study shows that with increase in the alkyl chain of the RTIL anion, single-phase region increases. Variation in chain length of RTIL anions is used for tuning the range of microemulsions area. Dynamic light scattering (DLS) measurements show that the hydrodynamic diameter (D_h) of both IL-in-oil microemulsions increases linearly with increase in R value. The difference in the extent of increase in size of microemulsions was found to be maximum in the case of $[C_2mim][C_4SO_4]$/[TX-100/cyclohexane. The octyl chain of the $[C_2mim][C_8SO_4]$ is aligned with the tail part of TX-100 molecules. But in the case of $[C_2mim][C_4SO_4]$, the butyl chain is apparently unsuccessful in functioning similarly and the ethyl sulfate anion is unable to form microemulsions in TX-100/cyclo-

dx.doi.org/10.1021/jp400013r | J. Phys. Chem. B XXXX, XXX, XXX−XXX

hexane system. So, we have used $[C_2mim][C_4SO_4]$-, $[C_2mim]$-$[C_6SO_4]$-, and $[C_2mim][C_8SO_4]$-containing microemulsions for solvent and rotational relaxation study using C-480 as molecular probe. The average solvation and rotational relaxation time of C-480 increases with increase in alkyl chain length of RTIL. The average solvation time decreases with increase in R values, due to the movement of C-480 molecules from the interfacial region to the polar core of microemulsions. Among these three microemulsions, the most pronounced change in solvent and rotational relaxation of C-480 is observed in the case of $[C_2mim][C_4SO_4]$/TX-100/cyclohexane microemulsions. Solvation times of C-480 largely depend on the size of microemulsions.

■ ASSOCIATED CONTENT

Supporting Information

Information on turbidity measurement, change in absorption spectra of C-480 at different R value, anisotropy decay of C-480 in neat $[C_2mim][C_8SO_4]$, neat $[C_2mim][C_4SO_4]$, TX-100/cyclohexane mixture, solvent correlation function, $C(t)$, and anisotropy decay of $[C_2mim][C_6SO_4]$/TX-100/cyclohexane, fluorescence decays of C-480 at R = 0.16, and time-resolved emission spectra (TRES) for $[C_2mim][C_4SO_4]$/TX-100/cyclohexane and $[C_2mim][C_8SO_4]$/TX-100/cyclohexane microemulsions. This material is available free of charge via the Internet at http://pubs.acs.org.

■ AUTHOR INFORMATION

Corresponding Author

*E-mail: nilmoni@chem.iitkgp.ernet.in. Phone: + 91-3222-283332.

Notes

The authors declare no competing financial interest.

■ ACKNOWLEDGMENTS

N.S. is thankful to the Council of Scientific and Industrial Research (CSIR), Government of India, for generous research grants. S.G., S.M., and V.G.R. are thankful to CSIR for research fellowship. C.B. is thankful to UGC for research fellowship.

■ REFERENCES

(1) Wagner, G. W.; Procell, L. R.; Yang, Y.-C.; Bunton, C. A. Molybdate/Peroxide Oxidation of Mustard in Microemulsions. *Langmuir* **2001**, *17*, 4809−4811.

(2) Moniruzzaman, M.; Tamura, M.; Tahara, Y.; Kamiya, N.; Goto, M. Ionic Liquid-in-Oil Microemulsion as a Potential Carrier of Sparingly Soluble Drug: Characterization and Cytotoxicity Evaluation. *Int. J. Pharm.* **2010**, *400*, 243−250.

(3) Bonini, M.; Bardi, U.; Berti, D.; Neto, C.; Baglioni, P. A New Way to Prepare Nanostructured Materials: Flame Spraying of Microemulsions. *J. Phys. Chem. B* **2002**, *106*, 6178−6183.

(4) Setua, P.; Pramanik, R.; Sarkar, S.; Ghatak, C.; Rao, V. G.; Sarkar, N.; Das, S. K. Synthesis of Silver Nanoparticle in Imidazolium and Pyrolidium Based Ionic Liquid Reverse Micelles: A step Forward in Nanostructure Inorganic Material in Room Temperature Ionic Liquid Field. *J. Mol. Liq.* **2011**, *162*, 33−37.

(5) Tang, S.; Baker, G. A.; Zhao, H. Ether-and Alcohol-Functionalizes Task-Specific Ionic Liquids: Attractive Properties and Applications. *Chem. Soc. Rev.* **2012**, *41*, 4030−4066.

(6) Mandal, D.; Datta, A.; Pal, S. K.; Bhattacharyya, K. Solvation Dynamics of 4-Aminophthalimide in Water-in-Oil Microemulsion of Triton X-100 in Mixed Solvents. *J. Phys. Chem. B* **1998**, *102*, 9070−9073.

(7) Sarkar, N.; Das, K.; Datta, A.; Das, S.; Bhattacharyya, K. Solvation Dynamics of Coumarin 480 in Reverse Micelles. Slow Relaxation of Water Molecules. *J. Phys. Chem.* **1996**, *100*, 10523−10527.

(8) Agazzi, F. M.; Falcone, R. D.; Silber, J. J.; Correa, N. M. Solvent Blends Can Control Cationic Reversed Micellar Interdroplet Interactions. The Effect of n-Heptane: Benzene Mixture on BHDC Reversed Micellar Interfacial Properties: Droplet Sizes and Micropolarity. *J. Phys. Chem. B* **2011**, *115*, 12076−12084.

(9) Baruah, B.; Roden, J. M.; Sedgwick, M.; Correa, N. M.; Crans, D. C.; Levinger, N. E. When Is Water Not Water? Exploring Water Confined in Large Reverse Micelles Using a Highly Charged Inorganic Molecular Probe. *J. Am. Chem. Soc.* **2006**, *128*, 12758−12765.

(10) Shirota, H.; Horie, K. Solvation Dynamics in Nonaqueous Reverse Micelles. *J. Phys. Chem. B* **1999**, *103*, 1437−1443.

(11) Correa, N. M.; Pires, P. A. R.; Silber, J. J.; El Seoud, A.; Real, O. Structure of Formamide Entrapped by AOT Nonaqueous Reverse Micelles: FT-IR and ^{1}H NMR Studies. *J. Phys. Chem. B* **2005**, *109*, 21209−21219.

(12) Chakraborty, A.; Seth, D.; Setua, P.; Sarkar, N. Dynamics of Solvent and Rotational Relaxation of Glycerol in the Nanocavity of Reverse Micelles. *J. Phys. Chem. B* **2006**, *110*, 5359−5366.

(13) Riter, R. E.; Undiks, E. P.; Kimmel, J. R.; Levinger, N. E. Formamide in Reverse Micelles: Restricted Environment Effects on Molecular Motion. *J. Phys. Chem. B* **1998**, *102*, 7931−7938.

(14) Shirota, H.; Segawa, H. Solvation Dynamics of Formamide and N, N-Dimethylformamide in Aerosol OT Reverse Micelles. *Langmuir* **2004**, *20*, 329−335.

(15) Welton, T. Ionic Liquids in Catalysis. *Coord. Chem. Rev.* **2004**, *248*, 2459−2477.

(16) Hallett, J. P.; Welton, T. Room-Temperature Ionic Liquids: Solvents for Synthesis and Catalysis. 2. *Chem. Rev.* **2011**, *111*, 3508−3576.

(17) Smiglak, M.; Metlen, A.; Rogers, R. D. The Second Evolution of Ionic Liquids: From Solvents and Separations to Advanced Materials-Energetic Examples from the Ionic Liquid Cookbook. *Acc. Chem. Res.* **2007**, *40*, 1182−1192.

(18) Dupont, J.; de Souza, R. F.; Suarez, P. A. Z. Ionic Liquid (Molten Salt) Phase Organometallic Catalysis. *Chem. Rev.* **2002**, *102*, 3667−3691.

(19) Gao, H. X.; Li, J. C.; Han, B. X.; Chen, W. N.; Zhang, J. L.; Zhang, R.; Yan, D. D. Microemulsions With Ionic Liquid Polar Domains. *Phys. Chem. Chem. Phys.* **2004**, *6*, 2914−2916.

(20) Eastoe, S.; Gold, S. E.; Rogers, A.; Paul, T.; Welton, R. K.; Heenan, I. G. Ionic Liquid-in-Oil Microemulsions. *J. Am. Chem. Soc.* **2005**, *127*, 7302−7303.

(21) Gao, Y.; Han, S.; Han, B.; Li, G.; Shen, D.; Li, Z.; Du, J.; Hou, W.; Zhang, G. TX-100/Water/1-Butyl-3-Methylimidazolium Hexafluorophosphate Microemulsions. *Langmuir* **2005**, *21*, 5681−5684.

(22) Anderson, J. L.; Pino, V.; Hagberg, E. C.; Sheares, V. V.; Armstrong, D. W. Surfactant Solvation Effects and Micelle Formation in Ionic Liquids. *Chem. Commun.* **2003**, 2444−2445.

(23) Fletcher, K. A.; Pandey, S. Surfactant Aggregation within Room-Temperature Ionic Liquid 1-Ethyl-3-Methylimidazolium Bis-(trifluoromethylsulfonyl)imide. *Langmuir* **2004**, *20*, 33−36.

(24) Zech, O.; Thomaier, S.; Bauduin, P.; Rück, T.; Touraud, D.; Kunz, W. Microemulsions with an Ionic Liquid Surfactant and Room Temperature Ionic Liquids As Polar Pseudo-Phase. *J. Phys. Chem. B* **2009**, *113*, 465−473.

(25) Rao, K. S.; Singh, T.; Trivedi, T. J.; Kumar, A. Aggregation Behavior of Amino Acid Ionic Liquid Surfactants in Aqueous Media. *J. Phys. Chem. B* **2011**, *115*, 13847−13853.

(26) Gao, Y.; Li, N.; Hilfert, L.; Zhang, S.; Zheng, L.; Yu, L. Temperature-Induced Microstructural Changes in Ionic Liquid-Based Microemulsions. *Langmuir* **2009**, *25*, 1360−1365.

(27) Pramanik, R.; Sarkar, S.; Ghatak, C.; Rao, V. G.; Sarkar, N. Ionic Liquid Containing Microemulsions: Probe by Conductance, Dynamic Light Scattering, Diffusion-Ordered Spectroscopy NMR Measurements, and Study of Solvent Relaxation Dynamics. *J. Phys. Chem. B* **2011**, *115*, 2322−2330.

(28) Porada, J. H.; Mansueto, M.; Laschat, S.; Stubenrauch, C. Microemulsions with Novel Hydrophobic Ionic Liquids. *Soft Matter* **2011**, *7*, 6805−6810.
(29) Ferreyra, D. D.; Correa, N. M.; Silber, J. J.; Falcone, R. D. The effect of Different Interfaces and Confinement on the Structure of the Ionic Liquid 1-Butyl-3-Methylimidazolium Bis-(trifluoromethylsulfonyl)imide Entrapped in Cationic and Anionic Reverse Micelles. *Phys. Chem. Chem. Phys.* **2012**, *14*, 3460−3470.
(30) Rao, V. G.; Ghosh, S.; Ghatak, C.; Mandal, S.; Brahmachari, U.; Sarkar, N. Designing a New Strategy for the Formation of IL-in-Oil Microemulsions. *J. Phys. Chem. B* **2012**, *116*, 2850−2855.
(31) Cheng, S.; Zhang, J.; Zhang, Z.; Han, B. Novel Microemulsions: Ionic Liquid-in-Ionic Liquid. *Chem. Commun.* **2007**, 2497−2499.
(32) Takahashi, K.; Sakai, S.; Tezuka, H.; Heijima, Y.; Katsumura, Y.; Watanabe, M. Reaction between Diiodide Anion Radicals in Ionic Liquids. *J. Phys. Chem. B* **2007**, *111*, 4807−4811.
(33) Reichardt, C. Polarity of Ionic Liquids Determined Empirically by Means of Solvatochromic Pyridinium N-Phenolate Betaine Dyes. *Green Chem.* **2005**, *7*, 339−351.
(34) Paul, A.; Samanta, A. Solute Rotation and Solvation Dynamics in an Alcohol-Functionalized Room Temperature Ionic Liquid. *J. Phys. Chem. B* **2007**, *111*, 4724−4731.
(35) Arzhantsev, S.; Jin, H.; Baker, G. A.; Maroncelli, M. Measurements of the Complete Solvation Response in Ionic Liquids. *J. Phys. Chem. B* **2007**, *111*, 4978−4989.
(36) Hu, Z.; Margulis, C. J. Room-Temperature Ionic Liquids: Slow Dynamics, Viscosity, and the Red Edge Effect. *Acc. Chem. Res.* **2007**, *40*, 1097−1105.
(37) Chakrabarty, D.; Seth, D.; Chakraborty, A.; Sarkar, N. Dynamics of Solvation and Rotational Relaxation of Coumarin 153 in Ionic Liquid Confined Nanometer-Sized Microemulsions. *J. Phys. Chem. B* **2005**, *109*, 5753−5758.
(38) Sasmal, D. K.; Mojumdar, S. S.; Adhikari, A.; Bhattacharyya, K. Deuterium Isotope Effect on Femtosecond Solvation Dynamics in an Ionic Liquid Microemulsion: An Excitation Wavelength Dependence Study. *J. Phys. Chem. B* **2010**, *114*, 4565−4571.
(39) Ghosh, S.; Mandal, S.; Banerjee, C.; Rao, V. G.; Sarkar, N. Photophysics of 3,3′-Diethyloxadicarbocyanine Iodide (DODCI) in Ionic Liquid Micelle and Binary Mixtures of Ionic Liquids: Effect of Confinement and Viscosity on Photoisomerization Rate. *J. Phys. Chem. B* **2012**, *116*, 9482−9491.
(40) Rabe, C.; Koetz, J. CTAB-Based Microemulsions with Ionic Liquids. *J. Colloids Surf., A* **2010**, *354*, 261−267.
(41) Wang, T.; Peng, C.; Liu, H.; Hu, Y. Phase behavior and Microstructure of the System Consisting of 1-Butyl-3-Methylimidazolium Hexafluorophosphate, Water, Triblock Copolymer F127 and Short-Chain Alcohols. *J. Mol. Liq.* **2009**, *146*, 89−94.
(42) Wei, J.; Su, B.; Yang, J.; Xing, H.; Bao, Z.; Yang, Y.; Ren, Q. Water Solubilization Capacity and Volume-Induced Percolation of Sodium Bis(2-ethylhexyl)sulfosuccinate Microemulsions in the Presence of 1-Alkyl-3-Methylimidazolium Chloride Ionic Liquids. *J. Chem. Eng. Data* **2011**, *56*, 3698−3702.
(43) Behera, K.; Om, H.; Pandey, S. Modifying Properties of Aqueous Cetyltrimethylammonium Bromide with External Additives: Ionic Liquid 1-Hexyl-3-methylimidazolium Bromide versus Cosurfactant n-Hexyltrimethylammonium Bromide. *J. Phys. Chem. B* **2009**, *113*, 786−793.
(44) Behera, K.; Dahiya, P.; Pandey, S. Effect of Added Ionic Liquid on Aqueous Triton X-100 Micelles. *J. Colloid Interface Sci.* **2007**, *307*, 234−245.
(45) Rao, V. G.; Ghatak, C.; Ghosh, S.; Mandal, S.; Sarkar, N. The Chameleon-Like Nature of Zwitterionic Micelles: The Effect of Ionic Liquid Addition on the Properties of Aqueous Sulfobetaine Micelles. *ChemPhysChem.* **2012**, *13*, 1893−1901.
(46) Tamoto, Y.; Segawa, H.; Shirota, H. Solvation Dynamics in Aqueous Anionic and Cationic Micelle Solutions: Sodium Alkyl Sulfate and Alkyltrimethylammonium Bromide. *Langmuir* **2005**, *21*, 3757−3764.
(47) Sarkar, N.; Dutta, A.; Das, S.; Bhattacharyya, K. Solvation Dynamics of Coumarin 480 in Micelles. *J. Phys. Chem.* **1996**, *100*, 15483−15486.
(48) Nandi, N.; Bagchi, B. Anomalous Dielectric Relaxation of Aqueous Protein Solutions. *J. Phys. Chem. A* **1998**, *102*, 8217−8221.
(49) Nandi, N.; Bhattacharyya, K.; Bagchi, B. Dielectric Relaxation and Solvation Dynamics of Water in Complex Chemical and Biological System. *Chem. Rev.* **2000**, *100*, 2013−2045.
(50) Pal, S. K.; Zewail, A. H. Dynamics of Water in Biological Recognition. *Chem. Rev.* **2004**, *104*, 2099−2124.
(51) Pramanik, R.; Ghatak, C.; Rao, V. G.; Sarkar, S.; Sarkar, N. Room Temperature Ionic Liquid in Confined Media: A Temperature Dependence Solvation Study in [bmim][BF_4]/BHDC/Benzene Reverse Micelles. *J. Phys. Chem. B* **2011**, *115*, 5971−5979.
(52) Willard, D. M.; Riter, R. E.; Levinger, N. E. Dynamics of Polar Solvation in Lecithin/Water/Cyclohexane Reverse Micelles. *J. Am. Chem. Soc.* **1998**, *120*, 4151−4160.
(53) Karmakar, R.; Samanta, A. Solvation Dynamics of Coumarin-153 in a Room-Temperature Ionic Liquid. *J. Phys. Chem. A* **2002**, *106*, 4447−4452.
(54) Saha, S.; Mandal, P. K.; Samanta, A. Solvation Dynamics of Nile Red in a Room Temperature Ionic Liquid Using Streak Camera. *Phys. Chem. Chem. Phys.* **2004**, *6*, 3106−3110.
(55) Mandal, P. K.; Samanta, A. Fluorescence Studies in a Pyrrolidinium Ionic Liquid: Polarity of the Medium and Solvation Dynamics. *J. Phys. Chem. B* **2005**, *109*, 15172−15177.
(56) Samanta, A. Solvation Dynamics in Ionic Liquids: What We Have Learned from the Dynamic Fluorescence Stokes Shift Studies. *J. Phys. Chem. Lett.* **2010**, *1*, 1557−1562.
(57) Kobrak, M. N. Characterization of the Solvation Dynamics of an Ionic Liquid via Molecular Dynamics Simulation. *J. Chem. Phys.* **2006**, *125*, 064502−064513.
(58) Jeong, D.; Shim, Y.; Choi, M. Y.; Kim, H. J. Effects of Solute Electronic Polarizability on Solvation in a Room-Temperature Ionic Liquid. *J. Phys. Chem. B* **2007**, *111*, 4920−4925.
(59) Bhargava, B. L.; Balasubramanian, S. Dynamics in a Room-Temperature Ionic Liquid: A Computer Simulation Study of 1, 3-Dimethylimidazolium Chloride. *J. Chem. Phys.* **2006**, *123*, 14505−14513.
(60) Huang, X. H.; Margulis, C. J.; Li, Y. H.; Berne, B. J. Why Is the Partial Molar Volume of CO_2 So Small When Dissolved in a Room Temperature Ionic Liquid? Structure and Dynamics of CO_2 Dissolved in [$Bmim^+$] [PF_6^-]. *J. Am. Chem. Soc.* **2005**, *127*, 17842−17851.
(61) Liu, X.; Zhou, G.; Zhang, S.; Wu, G.; Yu, G. Molecular Simulation of Guanidinium-Based Ionic Liquids. *J. Phys. Chem. B* **2007**, *111*, 5658−5668.
(62) Kashyap, H. K.; Biswas, R. Dipolar Solvation Dynamics in Room Temperature Ionic Liquids: An Effective Medium Calculation Using Dielectric Relaxation Data. *J. Phys. Chem. B* **2008**, *112*, 12431−12438.
(63) Kashyap, H. K.; Biswas, R. Solvation Dynamics of Dipolar Probes in Dipolar Room Temperature Ionic Liquids: Separation of Ion-Dipole and Dipole-Dipole Interaction Contributions. *J. Phys. Chem. B* **2010**, *114*, 254−268.
(64) Hazra, P.; Chakrabarty, D.; Sarkar, N. Solvation Dynamics of Coumarin 153 in Aqueous and Non-Aqueous Reverse Micelles. *Chem. Phys. Lett.* **2003**, *371*, 553−562.
(65) Falcone, R. D.; Correa, N. M.; Silber, J. J. On the Formation of New Reverse Micelles: A Comparative Study of Benzene/Surfactants/Ionic Liquids Systems Using UV-Visible Absorption Spectroscopy and Dynamic Light Scattering. *Langmuir* **2009**, *25*, 10426−10429.
(66) Maroncelli, M.; Fleming, G. R. Picosecond Solvation Dynamics of Coumarin 153: The Importance of Molecular Aspects of Solvation. *J. Chem. Phys.* **1987**, *86*, 6221−6239.
(67) Jin, H.; Baker, G. A.; Arzhantsev, S.; Dong, J.; Maroncelli, M. Solvation and Rotational Dynamics of Coumarin 153 in Ionic Liquids: Comparisons to Conventional Solvents. *J. Phys. Chem. B* **2007**, *111*, 7291−7302.

(68) Chapman, C. F.; Maroncelli, M. Fluorescence Studies of Solvation and Solvation Dynamics in Ionic Solutions. *J. Phys. Chem.* **1991**, *95*, 9095−9114.
(69) Headley, L. S.; Mukherjee, P.; Anderson, J. L.; Ding, R.; Halder, M.; Armstrong, D. W.; Song, X.; Petrich, J. W. Dynamic Solvation in Imidazolium-Based Ionic Liquids on Short Time Scales. *J. Phys. Chem. A* **2006**, *110*, 9549−9554.
(70) Bose, S.; Adhikary, R.; Mukherjee, P.; Song, X.; Petrich, J. W. Considerations for the Construction of the Solvation Correlation Function and Implications for the Interpretation of Dielectric Relaxation in Proteins. *J. Phys. Chem. B* **2009**, *113*, 11061−11068.
(71) Mukherjee, P.; Crank, J. A.; Sharma, P. S.; Wijeratne, A. B.; Adhikary, R.; Bose, S.; Armstrong, D. W.; Petrich, J. W. Dynamic Solvation in Phosphonium Ionic Liquids: Comparison of Bulk and Micellar Systems and Considerations for the Construction of the Solvation Correlation Function C(t). *J. Phys. Chem. B* **2008**, *112*, 3390−3396.
(72) Castner, E. W., Jr.; Wishart, J. F.; Shirota, H. Intermolecular Dynamics, Interactions, and Solvation in Ionic Liquids. *Acc. Chem. Res.* **2007**, *40*, 1217−1227.
(73) Samanta, A. Dynamic Stokes Shift and Excitation Wavelength Dependent Fluorescence of Dipolar Molecules in Room Temperature Ionic Liquids. *J. Phys. Chem. B* **2006**, *110*, 13704−13716.
(74) Shirota, H.; Tamoto, Y.; Segawa, H. Dynamic Fluorescence Probing of the Microenvironment of Sodium Dodecyl Sulfate Micelle Solutions: Surfactant Concentration Dependence and Solvent Isotope Effect. *J. Phys. Chem. A* **2004**, *108*, 3244−3252.
(75) Fee, R. S.; Maroncelli, M. Estimating the Time-Zero Spectrum in Time-Resolved Emission Measurements of Solvation Dynamics. *Chem. Phys.* **1994**, *183*, 235−247.